New Methods for Simulation of Fractional Brownian Motion

Z.-M. YIN

*Pacific Geoscience Centre, Geological Survey of Canada, Sidney, British Columbia, Canada V8L 4B2; School of Earth and Ocean Sciences,
University of Victoria, Victoria, British Columbia, Canada V8W 2Y2*

We present new algorithms for simulation of fractional Brownian motion (fBm) which comprises a set of important random functions widely used in geophysical and physical modeling, fractal image (landscape) simulating, and signal processing. The new algorithms, which are both accurate and efficient, allow us to generate not only a one-dimensional fBm process, but also two- and three-dimensional fBm fields. © 1996 Academic Press, Inc.

1. INTRODUCTION

Fractional Brownian motion (fBm) comprises a family of random functions described by index H ($0 < H < 1$). The earliest mention of them in literature could date back to 1940 [1]. These random functions were given a name ''fractional Brownian motion'' by Mandelbrot and van Ness [2] and joined the fractal family created by Mandelbrot [3]. In recent years, fBm has found applications in many physical sciences and engineering, such as simulation of landscape and seafloor topography [4, pp. 247–276; 5–6], geophysical modeling [7–9], and signal processing [10]. Thus, developing a good simulation algorithm for fBm is of not only theoretical, but also practical, importance.

Although a number of simulation algorithms have been proposed, none of them are satisfactory in terms of the dual criteria ''accuracy and efficiency.'' Among the existing algorithms, two commonly used algorithms are midpoint displacement and Fourier filtering methods [11, pp. 82–109]. The midpoint displacement method proposed by Fournier *et al.* [12] needs little computing time to generate a realization and is an efficient algorithm. However, as criticized by Mandelbrot [13], this algorithm does not lead to a process that has stationary increments. The process generated by this method is therefore no true fBm. The Fourier filtering method is based on the spectral property of fBm. It uses the Fourier transform to generate a process that has a spectral density $S(f) \propto f^{(1+2H)}$ [11, pp. 93–94, 105–109]. However, this power law relation $S(f) \propto f^{(1+2H)}$ is derived by time (or spatial) average and is therefore an approximation, because fBm is non-stationary and does not possess a time- (or spatial) independent spectrum. This

approximation is good only if the frequency (f) is relatively large [14, pp. 155–158, 247]. Consequently, inaccuracy in simulation of fBm, resulting from the Fourier filtering methods is inevitable (see [11, pp. 82–109] for general discussion). Besides, Felder [15, pp. 172–174] proposed an algorithm which is based on Mandelbrot and von Ness' work [2]. This algorithm can simulate accurately one-dimensional fBm, but it is very time-consuming.

The purpose of this paper is to develop both accurate and efficient methods for simulation of one- and two-dimensional fBm. We also deal with the three-dimensional simulation.

2. SPECTRAL METHOD FOR ONE-DIMENSIONAL SIMULATION

The one-dimensional fBm with index H ($0 < H < 1$) is defined as [4, pp. 350–352; 14, p. 246; 15, p. 170]: (1) $B_H(x)$ is continuous and $B_H(0) = 0$ with probability $P = 1$; (2) for any $x \geq 0$ and $r \geq 0$, the increment $B_H(x + r) - B_H(x)$ follows the normal distribution with zero mean and variance $r_0 r^{2H}$, that is

$$
P\{B_H(x + r) - B_H(x) \leq z\}
$$
$$
= \frac{1}{\sqrt{2\pi r_0} r^H} \int_{-\infty}^{z} \exp\left(-\frac{u^2}{2r_0 r^{2H}}\right) du, \tag{1}
$$

where r_0 is a constant. The argument x represents either time or spatial parameter. When $H = 1/2$, fBm reduces to ordinary Brownian motion. The autocovariance function of fBm is [16, p. 407]

$$
\text{cov}\{B_H(x), B_H(x + r)\}
$$
$$
= \frac{r_0}{2}[x^{2H} + (x + r)^{2H} - |r|^{2H}], \quad x \geq 0, x + r \geq 0. \tag{2}
$$

In devising an algorithm, all the previous methods deal directly with fBm itself. This makes the simulation complicated because of fBm's non-stationary property. In this

66

paper, we change the strategy. We deal directly with fBm's increments. The reason to do this is very simple. fBm has stationary increments, and the increments themselves comprise a discrete stationary process. It is much easier to simulate a stationary process than to simulate a nonstationary process. Dealing with the increments makes it possible to devise an algorithm that is both accurate and efficient. The increment of fBm is defined as

$$W_H(x) = B_H(x + \Delta x) - B_H(x), \quad x \geq 0. \tag{3}$$

We term $W_H(x)$ fractional white noise, since when $H = \frac{1}{2}$ $W_H(x)$ reduces to ordinary white noise. $W_H(x)$ is a discrete stationary process with zero mean and variance $r_0 \Delta x^{2H}$. Instead of simulating fBm directly, we simulate the fractional white noise $W_H(x)$. Then, fBm with index H can be obtained by summation of the fractional white noise with the same index H, which is similar to the simulation of the ordinary Brownian motion by summation of the white noise.

When first looking at Eq. (3), it seems that Δx (increment in x) determines the resolution of simulation, and different Δx should be used to generate a process with different resolutions. In fact, the process with any resolution can be simulated using the same Δx. This is because the paths of fBm are self-affine fractals and scale invariant. The two processes $B_H(x)$ and $B_H(\tau x)/\tau^H$ (where τ is a constant) are statistically identical. Therefore, the process with any resolution can be obtained, once $B_H(x)$ is simulated. Here, we set $\Delta x = 1$ and generate a process in which x takes only integers, 0, 1, 2, ..., N.

The autocovariance function of $W_H(x)$ can be derived from Eq. (2),

$$\begin{aligned}
C(r) &= \text{cov}\,\{W_H(x), W_H(x + r)\} \\
&= E[\{B_H(x + 1) - B_H(x)\}\{B_H(x + r + 1) - B_H(x + r)\}] \\
&= \frac{r_0}{2}\,(|r + 1|^{2H} + |r - 1|^{2H} - 2|r|^{2H}), \quad r = 0, \pm 1, \pm 2, ...,
\end{aligned}$$
$$\tag{4}$$

Where E is the expectation operator. Since $W_H(x)$ is a stationary and discrete process, its power spectral density function is [17, p. 225]

$$S(f) = \sum_{r=-\infty}^{\infty} C(r) \cos(2\pi rf), \quad -\frac{1}{2} \leq f \leq \frac{1}{2}, \tag{5}$$

where f denotes frequency (in hertz) or spatial frequency. The autocovariance function $C(r)$ may be represented by the inverse Fourier transform of $S(f)$ [17, p. 225]:

$$C(r) = \int_{-1/2}^{1/2} S(f) \cos(2\pi rf)\,df, \quad r = 0, \pm 1, \pm 2, ... \tag{6}$$

The spectral density and the autocovariance function of a stationary process are mutually representable in terms of the Fourier transform pair, such as shown in Eqs. (5) and (6) for the discrete case. Consequently, given the spectral density function, a process can be easily generated using any spectral method. Here we use the classical method proposed by Rice [18] and modified by Shinozuka and Jan [19]. We rewrite the expression as

$$\begin{aligned}
W_H(x) &= \sqrt{2} \sum_{k=-N/2}^{N/2-1} [S(f_k)\,\Delta f]^{1/2} \cos(2\pi f_k x + \phi_k), \\
& x = 0, 1, 2, ..., N,
\end{aligned}$$
$$\tag{7}$$

where $S(f)$ is the spectral density function given by Eq. (5), N is the total number of sampling in f, $\Delta f = 1/N$ is the interval of sampling, $f_k = k\,\Delta f$ are the values of f sampled, and ϕ_k are independent random angles uniformly distributed between 0 and 2π. Wang [20] recognized that Eq. (7) could be calculated using a fast Fourier transform (FFT). Expanding the cosine function on the right-hand side of Eq. (7), we obtain

$$\begin{aligned}
W_H(x) &= \sqrt{2/N} \sum_{k=-N/2}^{N/2-1} \left[S\left(\frac{k}{N}\right) \right]^{1/2} \left[\cos(\phi_k) \cos\left(\frac{2\pi kx}{N}\right) \right. \\
& \left. - \sin(\phi_k) \sin\left(\frac{2\pi kx}{N}\right) \right], \quad x = 0, 1, 2, ..., N.
\end{aligned}$$
$$\tag{8}$$

It is evident that Eq. (8) can be calculated using a complex FFT algorithm. If one inputs $[S(k/N)]^{1/2} \cos(\phi_k)$ as the real part and $[S(k/N)]^{1/2} \sin(\phi_k)$ as the imaginary part of input complex data, then the real part of output complex data is $W_H(x)$.

It is easy to prove that the autocovariance function of a process simulated by Eq. (8) converges to the theoretical one. Let $C_s(r)$ denote the autocovariance function of the simulated process, it follows from Eq. (7) that

$$\begin{aligned}
C_s(r) &= E[W_H(x), W_H(x + r)] \\
&= 2 \sum_{k=-N/2}^{N/2-1} S(f_k)\,\Delta f \\
& E[\cos(2\pi f_k x + \phi_k) \cos(2\pi f_k(x + r) + \phi_k)] \\
&= \sum_{k=-N/2}^{N/2-1} S(f_k)\,\Delta f \cos(2\pi f_k r),
\end{aligned}$$
$$\tag{9}$$

noting that ϕ_k are independent random variables and follow the uniform distribution between 0 and 2π. Comparing Eqs. (6) and (9) and taking the limit $N \to \infty$, one obtains
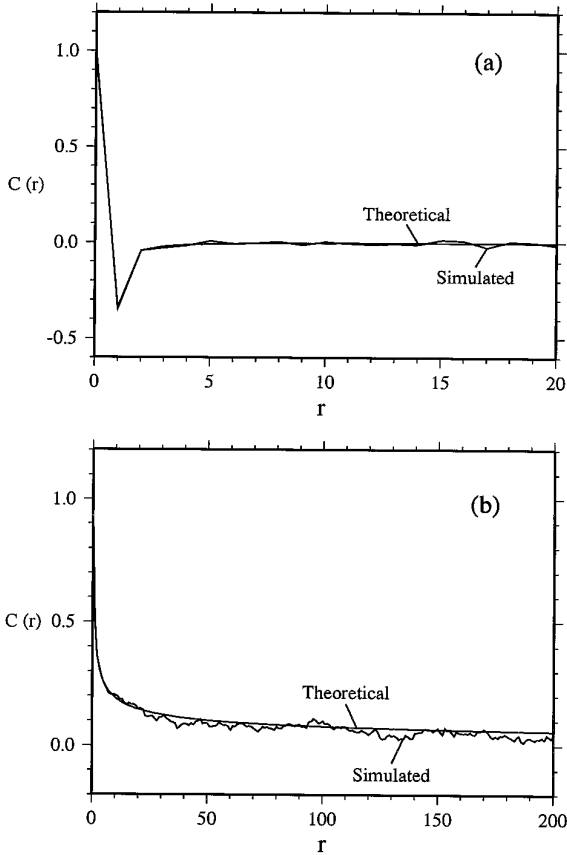
FIG. 1. Comparison between theoretical autocovariance of the fractional white noise and sample autocovariance calculated using "time" average of a single realization simulated by the spectral method: (a) Index $H = 0.2$; (b) $H = 0.8$.

$$\lim_{N \to \infty} C_s(r) = \int_{-1/2}^{1/2} S(f) \cos (2\pi rf) \, df = C(r). \quad (10)$$

Shinozuka and Jan [19] have proven that the rate of convergence to the theoretical autocovariance function is about $1/N^2$, which is fast. As examples, we use Eq. (8) to simulate two $W_H(x)$ realizations with index $H = 0.2$ and 0.8, respectively (assume $r_0 = 1$). Both have length $N = 4096$. Figure 1 shows the comparison between the theoretical autocovariance calculated using Eq. (4) and the sample autocovariance calculated using "time" average of a single realization generated.

It should be pointed out that the summation in Eq. (5) converges only when $H \leq 1/2$. In the case of $H \leq 1/2$, one obtains a unique spectral density. This spectral density can be used to simulate processes with any length. In the case of $H > \frac{1}{2}$, the spectral density diverges for $|r| \to \infty$, but it converges for finite r. Since any simulation involves a finite length, one may calculate the spectral density function for finite r. The spectral density calculated are different for different ranges of r. Therefore, in order to avoid any

inaccuracy in simulation, the range of r should be chosen exactly the same as the length of $W_H(x)$ simulated. For instance, if one wants to generate a process with a length of $0 \leq x \leq N - 1$, the summation in Eq. (5) must be calculated over the range of $-N/2 \leq r \leq N/2 - 1$ (assume $C(r) = 0$ for $r > N/2 - 1$ and $r < -N/2$).

With an FFT algorithm, the evaluation of Eq. (8) requires of order $N \log_2 N$ operations to generate a series of N points of $W_H(x)$. Since the sample autocovariance function converges to the theoretical autocovariance function with a rate of $1/N^2$, the new method presented above is guaranteed to give rise to both accurate and fast simulation of one-dimensional fBm. As mentioned above, two commonly used simulation algorithms are the midpoint displacement and the Fourier filtering [11, pp. 82–109]. The midpoint displacement algorithm requires about N operations to generate a fBm process with a length N, which is very efficient. However, this algorithm is of very poor accuracy, because the process generated by it does not have stationary increments and is therefore not true fBm [13]. The Fourier filtering method also uses a FFT algorithm to simulate fBm. Thus, the operations required by this algorithm are the same as those required by the method presented in this paper, that is, about $N \log_2 N$ operations. The Fourier filtering algorithm has a shortcoming. It simulates fBm on the basis of the spectral property other than the autocovariance function of fBm. The algorithm generates a process that has a spectral density $S(f) \propto f^{(1+2H)}$. As addressed by Falconer [14, pp. 155–158, 247], this power law relation $S(f) \propto f^{(1+2H)}$ is derived by time (or spatial) average and is therefore an approximation, because fBm is non-stationary and does not possess a time- (or spatial) independent spectrum. This approximation is poor when the frequency (f) is very small. As a result, the deviation of the sample autocovariance function from the theoretical one increases with increasing correlation distance. Besides, the algorithm proposed by Felder [15, pp. 172–174] requires MN operations to generate a process of N discrete points. The simulation accuracy depends on the parameter M. To ensure a good simulation, $M \geq 700$ is usually chosen, which shows that this algorithm is inefficient. In summary, comparing the new algorithm with previous algorithms, when their efficiency is comparable, the new algorithm is more accurate, and when their accuracy is comparable, the new algorithm is more efficient.

3. TURNING BANDS METHOD FOR TWO-DIMENSIONAL SIMULATION

In analogy to the one-dimensional case, the two-dimensional fBm with stationary and isotropic increments can be defined as [16, pp. 441–442]: (1) $B_H(x_1, x_2)$ is continuous and $B_H(0, 0) = 0$ with probability $P = 1$; (2) for any $x_1 \geq$
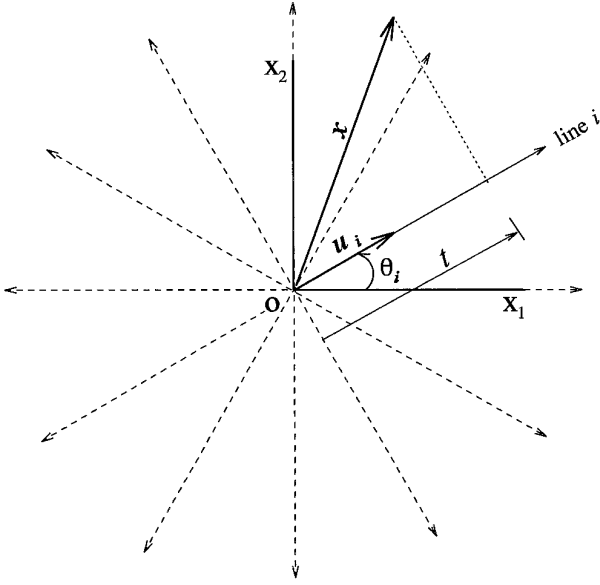
FIG. 2. Schematic representation of the turning bands method. $\mathbf{x}$ is a vector denoting a point on the field to be simulated and $\mathbf{u}_i$ is a unit vector on the line i. $t = \mathbf{x} \cdot \mathbf{u}_i$, denoting the position on the line at which the value of the one-dimensional process is added to the simulated field at the point $\mathbf{x}$. θ_i is the azimuth of line i, which is uniformly distributed from 0 to 2π. The two arrows on each line indicate that two identical one-dimensional realizations are connected at the origin o and toward opposite directions.

$0, x_2 \geq 0, r_1 \geq 0, r_2 \geq 0$, the increment $B_H(x_1 + r_1, x_2 + r_2) - B_H(x_1, x_2)$ follows the normal distribution with zero mean and variance $r_0 r^{2H}$, where $r = (r_1^2 + r_2^2)^{1/2}$ and r_0 is a constant.

The turning bands method, originally proposed by Matheron [21], was improved by Mantoglou and Wilson [22] to simulate multidimensional stationary random fields. It is a fast simulation algorithm. The fundamental of the turning bands method is to transform a multidimensional simulation into the sum of a series of equivalent one-dimensional simulations. Although in [22] the applicability of the turning bands method is restricted to stationary processes, we demonstrate here that it is also applicable to simulation of the two-dimensional non-stationary fBm.

With reference to Fig. 2, along each line we generate two identical one-dimensional realizations (the second one can be obtained by duplicating the first one), and we connect them at the origin (towards opposite directions). The simulated one-dimensional processes along different lines are independent. At this moment, we only assume that these one-dimensional processes are non-stationary with zero mean and stationary increments. Suppose that there are in total L lines which are uniformly distributed from 0 to 2π. We assign the two-dimensional field at a point x the value $B_H(x)$ given by

$$B_H(x) = \frac{1}{\sqrt{L}} \sum_{i=1}^{L} Z_i(\mathbf{x} \cdot \mathbf{u}_i), \quad (11)$$

where i is the ith line, $\mathbf{u}$ is a unit vector along the line, $\mathbf{x} \cdot \mathbf{u}_i$ denotes the projection of the vector $\mathbf{x}$ onto line i, and $Z(\mathbf{x} \cdot \mathbf{u})$ is the value of the simulated one-dimensional process at point $\mathbf{x} \cdot \mathbf{u}$.

Since the mean of the simulated one-dimensional process is zero, one can readily prove that the simulated two-dimensional field $B_H(x)$ has zero mean. Furthermore, because the lines are uniformly distributed from 0 to 2π, the increments of $B_H(x)$ are guaranteed to be isotropic. Now, a question that arises is "what is the one-dimensional process that can give rise to the known autocovariance function of two-dimensional fBm field?" Let $V_s(r)$ denote the variance of increments of the two-dimensional process simulated by the turning bands method. One can write from Eq. (11) that

$$V_s(r) = \frac{1}{L} E \left[\left\{ \sum_{i=1}^{L} [Z_i(\mathbf{x}_2 \cdot \mathbf{u}_i) - Z_i(\mathbf{x}_1 \cdot \mathbf{u}_i)] \right\}^2 \right], \quad (12)$$

where $r = |\mathbf{x}_2 - \mathbf{x}_1|$. Noting that the one-dimensional realizations along different lines are independent and assumed to have stationary increments, Eq. (12) reduces to

$$V_s(r) = \frac{1}{L} \sum_{i=1}^{L} E[\{Z_i(\mathbf{x}_2 \cdot \mathbf{u}_i) - Z_i(\mathbf{x}_1 \cdot \mathbf{u}_i)\}^2]$$

$$= \frac{1}{L} \sum_{i=1}^{L} V_1(\mathbf{h} \cdot \mathbf{u}_i), \quad (13)$$

where V_1 denotes the variance of increments of the one-dimensional process and $\mathbf{h} = \mathbf{x}_2 - \mathbf{x}_1$. Taking the limit $L \to \infty$ yields

$$V_2(r) = \lim_{L \to \infty} V_s(r)$$

$$= E[V_1(\mathbf{h} \cdot \mathbf{u})]$$

$$= \int_c V_1(\mathbf{h} \cdot \mathbf{u}) f(\mathbf{u}) \, d\mathbf{u},$$

where $V_2(r) = r_0 r^{2H}$ is the theoretical variance of increments of two-dimensional fBm ($r = |\mathbf{h}| = |\mathbf{x}_2 - \mathbf{x}_1|$), c denotes the unit circle, and $f(\mathbf{u})$ is the density function of $\mathbf{u}$. Since the lines in Fig. 2 are uniformly distributed from 0 to 2π, $f(\mathbf{u}) = 1/(2\pi)$. We define two orthogonal axes x and y with the origin at the point of $\mathbf{x}_1$ and the y-axis in the direction of the vector $\mathbf{h} = \mathbf{x}_2 - \mathbf{x}_1$. In polar coordinates, $\mathbf{h} \cdot \mathbf{u} = r \sin \theta$ and $d\mathbf{u} = d\theta$, we have

$$V_2(r) = \frac{1}{2\pi} \int_0^{2\pi} V_1(r \sin \theta) \, d\theta. \quad (15)$$

Changing the integral variable from θ to κ, where $\kappa = r \sin \theta$, and replacing $V_2(r)$ with $r_0 r^{2H}$, Eq. (15) becomes

$$\int_0^r \frac{V_1(\kappa)}{(r^2 - \kappa^2)^{1/2}} \, d\kappa = \frac{\pi}{2} r_0 r^{2H}. \tag{16}$$

This is a standard singular Volterra integral equation of the first kind, the solution of which can be found from text books, e.g., [23, pp. 172–173]. The solution is

$$V_1(\kappa) = \frac{\sqrt{\pi} \, \Gamma(1 + H)}{\Gamma(\frac{1}{2} + H)} r_0 \kappa^{2H}. \tag{17}$$

Eq. (17) shows that, in order to preserve the theoretical correlation for the two-dimensional fBm, the one-dimensional process to be simulated must be one-dimensional fBm, but with the variance of its increments multiplied by a factor which is a function of the index H. This result is not surprising, because any profile of two-dimensional fBm is one-dimensional fBm. The simulation technique for one-dimensional fBm has been discussed in the previous section. Therefore, to simulate the two-dimensional fBm, one just needs to change the autocovariance function given in Eq. (4) from $C(r)$ to $\pi^{1/2}\Gamma(1 + H)C(r)/\Gamma(1/2 + H)$ and generate some one-dimensional fBm realizations. A two-dimensional fBm realization with $r_0 r^{2H}$ (the variance of increments) can be obtained using the simple algorithm given in Eq. (11).

Errors in simulation using the turning bands method come from a number of sources, such as the finite number of lines (L), the error in simulation of one-dimensional fBm, and the discretization along the lines (band width). As mentioned above, the spectral method presented in this paper can simulate accurately one-dimensional process fBm, so the error resulting from the one-dimensional simulation is minor. The effect of the discretization along the lines on simulation accuracy has been discussed in [22], which is also applicable to the present case of simulating fBm. Here, we only discuss the effect of the number of lines on simulation accuracy. Mantoglou and Wilson [22] have found that evenly distributed lines give rise to a much faster rate of convergence to the target autocovariance than randomly distributed lines, so the approach of randomly generating lines is never used. Let ε be the variance error of increments for evenly distributed lines; it follows that

$$\begin{aligned} \varepsilon &= V_s(r) - V_2(r) \\ &= \frac{1}{L} \sum_{i=1}^L V_1(r \sin \theta_i) - \frac{1}{\pi} \int_0^\pi V_1(r \sin \theta) \, d\theta \\ &= \frac{1}{L} \sum_{i=1}^L V_1(r \sin \theta_i) - r_0 r^{2H}. \end{aligned} \tag{18}$$

Equation (18) shows that the error ε results from the approximation of integration by summation (or numerical
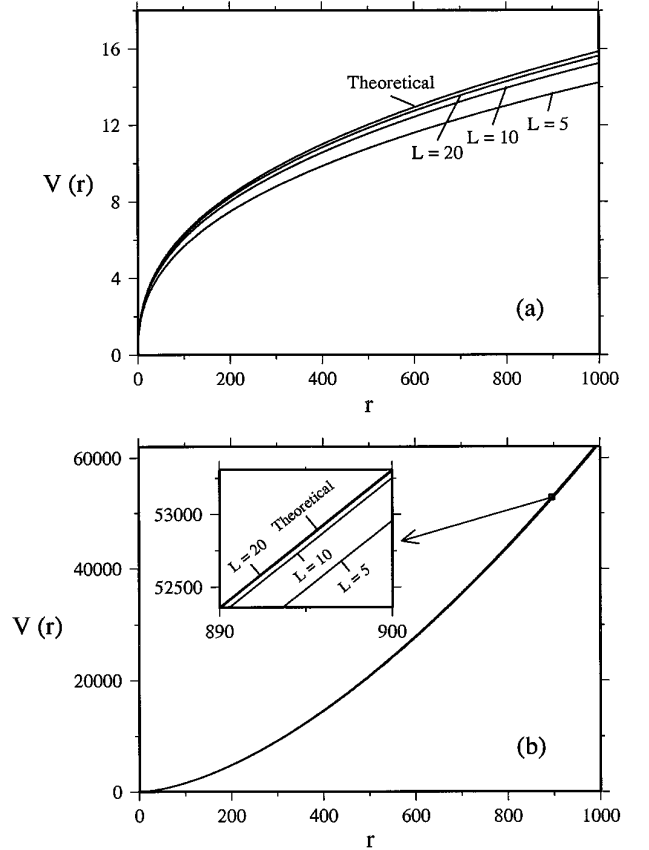

FIG. 3. Comparison between theoretical variance of increments of the two-dimensional fractional Brownian motion and variance of increments of the process simulated by the turning bands method using a different number of lines. The inset shows the details: (a) $H = 0.2$; (b) $H = 0.8$.

integration). The value of the summation is not only a function of distance r and the number of lines, but also affected by positions of the points $\mathbf{x}_1$ and $\mathbf{x}_2$ ($r = |\mathbf{x}_2 - \mathbf{x}_1|$). For this reason, the value of the summation may be slightly different for different positions of points lying the same distance r apart. In other words, the increments of the simulated two-dimensional field are not perfectly isotropic. It can be readily proven that the largest error occurs when the points lie on one of the lines, and the error is the smallest when the points lie on the bisector between two lines. Nevertheless, as the number of lines increases, the variance of increments of the simulated random field converges to the theoretical one, and the increments become isotropic. As examples, Fig. 3 shows the variance error of increments of the two-dimensional field calculated using Eq. (18) for the case where the points lie along a line. For both examples, as the number of lines increases, the variance of increments of the simulated process converges fast to the theoretical variance. As far as the number of lines is concerned, we find that, depending on the accuracy

desired, 20 lines should be sufficient to do a good simulation.

The Fourier filtering method is often used to simulate two-dimensional fBm [11, pp. 105–109]. Employing a FFT algorithm, this method requires $(N \log_2 N)^2$ operations to generate a two-dimensional fBm field of N by N discrete points. The cost for the turning bands method comprises mainly two parts: (1) generating line processes and (2) evaluating Eq. (11). The former requires $LN \log_2 N$ operations and the latter requires LN^2, where L represents the number of lines. Consequently, the total cost is of order LN^2. Since 20 lines ($L = 20$) are sufficient to do an accurate simulation. The turning bands method presented in this paper is superior to the Fourier filtering method in terms of both accuracy and efficiency.

4. TURNING BANDS METHOD FOR THREE-DIMENSIONAL SIMULATION

To date, only one- and two-dimensional fBm have found applications. However, if necessary, the aforementioned turning bands method can be easily extended to simulation of three-dimensional fBm field. The three-dimensional fBm can be defined as: (1) $B_H(x_1, x_2, x_3)$ is continuous and $B_H(0, 0, 0) = 0$ with probability $P = 1$; (2) for any $x_1 \geq 0$, $x_2 \geq 0$, $x_3 \geq 0$, $r_1 \geq 0$, $r_2 \geq 0$, and $r_3 \geq 0$, the increment $B_H(x_1 + r_1, x_2 + r_2, x_3 + r_3) - B_H(x_1, x_2, x_3)$ follows the normal distribution with zero mean and variance $r_0 r^{2H}$, where $r = (r_1^2 + r_2^2 + r_2^2)^{1/2}$ and r_0 is a constant.

To simulate the three-dimensional field, one just changes the distribution of lines in Fig. 2 from uniform distribution on the circle to approximately uniform distribution on the sphere (note that when L is outside the set $\{4, 6, 8, 12, 20\}$, a uniform distribution of points over the surface of a sphere does not exist; that is, the angle between any two lines cannot be made identical. One can only attempt to make the distribution of lines approximately uniform). The algorithm to assign the value of B_H at a point (x_1, x_2, x_3) is still the same as Eq. (11), and the expression for the variance of increments of the simulated field is similar to Eq. (13). Because the lines are approximately uniformly distributed on the sphere, the sensity function of $\mathbf{u}$ (unit vector on the lines) is $f(\mathbf{u}) = 1/(4\pi)$. It follows from Eq. (14) that

$$V_3(r) = \frac{1}{4\pi} \int_c V_1(\mathbf{h} \cdot \mathbf{u}) \, d\mathbf{u}, \qquad (19)$$

where c denotes the unit sphere. In analog to the two-dimensional analysis, we define orthogonal axes (x, y, z) with the origin at the point of $\mathbf{x}_1$ and with the z axis in the direction of the vector $\mathbf{h} = \mathbf{x}_2 - \mathbf{x}_1$. In spherical coordinates, we can write $\mathbf{h} \cdot \mathbf{u} = r \cos \phi$ (where $r = |\mathbf{h}|$), and $d\mathbf{u} = \sin \phi \, d\phi \, d\theta$. Then, Eq. (19) becomes

$$V_3(r) = \frac{1}{4\pi} \int_0^{2\pi} \int_0^{\pi} V_1(r \cos \phi) \sin \phi \, d\phi \, d\theta. \qquad (20)$$

Changing integral variables from θ and ϕ to θ and κ, where $\kappa = r \cos \phi$, and replacing $V_3(r)$ by $r_0 r^{2H}$ yields

$$\int_0^r V_1(\kappa) \, d\kappa = r_0 r^{2H+1}. \qquad (21)$$

This simple integral equation can be readily solved. The solution is $V_1(\kappa) = (2H + 1)r_0 \kappa^{2H}$, which shows that the one-dimensional process to be simulated must be the fBm with the variance of increments multiplied by a factor $2H + 1$.

Similar to the two-dimensional case, the simulation accuracy for the three-dimensional fBm depends on the number of lines (L), the accuracy in simulation of the one-dimensional fBm, and the resolution of discretization along the lines (band width). The variance error (ε) of the increments for evenly distributed lines can be expressed as

$$\varepsilon = V_s(r) - V_3(r)$$
$$= \frac{1}{L} \sum_{i=1}^{L} V_1(r \cos \phi_i) - r_0 r^{2H}. \qquad (22)$$

For the three-dimensional simulation, more lines are required to achieve the same simulation accuracy as that for the two-dimensional case.

CONCLUSIONS

In this paper, two new methods are proposed to simulate one-dimensional and multidimensional fBm. The main results can be summarized as follows:

(1)   The increments of one-dimensional fBm constitute a discrete stationary process, which is termed fractional white noise. Instead of simulating fBm directly, we propose a FFT algorithm (on the basis of a classical spectral method) to simulate the fractional white noise. Then fBm can be obtained by summation of the fractional white noise. The autocovariance function of the simulated process converges as $1/N^2$ to the theoretical one.

(2)   The turning bands method, which was used previously to simulate multidimensional stationary processes, is introduced to simulate two-dimensional non-stationary fBm. It is proven that, in order to preserve the known covariance function for the two-dimensional fBm, the line process in the turning bands method must be one-dimensional fBm with the variance multiplied by a factor. Thus, two-dimensional fBm can be simulated by the summation of a series of line processes, each of which is an independent

realization of one-dimensional fBm. The result shows that 20 lines are sufficient to do a good simulation.

(3)   It is proven that the turning bands method can also be applied to simulate three-dimensional fBm. The major differences between two- and three-dimensional simulation are: (a) the autocovariance of the line process is multiplied by different factors and (b) the lines are evenly distributed on the circle for the two-dimensional simulation and are approximately evenly distributed on the sphere for the three-dimensional simulation.

ACKNOWLEDGMENTS

REFERENCES

1. A. N. Kolmogorov, *Dokl. Akad. Nauk SSSR* **26,** 6 (1940).

2. B. B. Mandelbrot and J. W. van Ness, *SIAM Rev.* **10,** 422 (1968).

3. B. B. Mandelbrot, *Fractals, Form, Chance, and Dimension* (Freeman, San Francisco, 1977).

4. B. B. Mandelbrot, *The Fractal Geometry of Nature* (Freeman, San Francisco, 1982).

5. C. G. Fox and D. E. Hayes, *Rev. Geophys.* **23,** 1 (1985).

6. M. F. Goodchild, *Math. Geol.* **20,** 615 (1988)

7. J. Huang and D. L. Turcotte, *J. Geophys. Res.* **94,** 7491 (1989).

8. O. G. Jensen, J. P. Todoeschuk, D. J. Crossley, and M. Gregotski, *Non-Linear Variability in Geophysics, Scaling and Fractals,* edited by D. Schertzer and S. Lovejoy (Kluwer Academic, Dordrecht, 1991).

9. Z.-M. Yin and G. Ranalli, *Geophys. J. Int.,* **123,** 838 (1995).

10. N. J. Kasdin, *Proc. IEEE* **83,** 802 (1995).

11. D. Saupe, *The Science of Fractal Images,* edited by H.-O. Peitgen and D. Saupe (Springer-Verlag, New York, 1988).

12. A. Fournier, D. Fusell, and L. Carpenter, *Commun. ACM* **25,** 371 (1982).

13. B. B. Mandelbrot, *Commun. ACM* **25,** 581 (1982).

14. K. Falconer, *Fractal Geometry, Mathematical Foundations and Applications* (Wiley, Chichester, 1990).

15. J. Felder, *Fractals* (Plenum, New York, 1988).

16. A. M. Yaglom, *Correlation Theory of Stationary and Related Random Functions. I. Basic Results* (Springer-Verlag, New York, 1987).

17. M. B. Priestley, *Spectral Analysis and Time Series* (Academic Press, London, 1981).

18. S. O. Rice, *Selected Papers on Noise and Stochastic Processes,* edited by N. Wax (Dover, New York, 1954).

19. M. Shinozuka and C.-M. Jan, *J. Sound Vib.* **25,** 111 (1972).

20. K. Wang, *EOS* **71,** 633 (1990).

21. G. Matheron, *Adv. Appl. Probab.* **5,** 439 (1973).

22. A. Mantoglou and J. L. Wilson, *Water Resour. Res.* **18,** 1379 (1982).

23. R. P. Kanwal, *Linear Integral Equations, Theory and Technique* (Academic Press, London, 1971).